

Article

Improving the Endoprosthesis Design and the Postoperative Therapy as a Means of Reducing Complications Risks after Total Hip Arthroplasty

Valentin L. Popov ^{1,*}, Aleksandr M. Poliakov ² and Vladimir I. Pakhaliuk ^{2,*}¹ Institute of Mechanics, Technische Universität Berlin, 10623 Berlin, Germany² Polytechnic Institute, Sevastopol State University, 299053 Sevastopol, Russia; a.m.poljakov@sevsu.ru

* Correspondence: v.popov@tu-berlin.de (V.L.P.); pahaluk@sevsu.ru (V.I.P.); Tel.: +49-30-3142-1480 (V.L.P.); +7-978-7640-600 (V.I.P.)

Abstract: One of the most high-tech, efficient and reliable surgical procedures is Total Hip Arthroplasty (THA). Due to the increase in average life expectancy, it is especially relevant for older people suffering from chronic joint disease, allowing them to return to an active lifestyle. However, the rejuvenation of such a severe joint disease as osteoarthritis requires the search for new solutions that increase the lifespan of a Total Hip Replacement (THR). Current trends in the development of this area are primarily focused on the creation of new materials used in THR and methods for their processing that meet the requirements of biocompatibility, long-term strength, wear resistance and the absence of an immune system response aimed at rejection. This study is devoted to the substantiation of one of the possible approaches to increase the reliability and durability of THR, based on the improvement of the implant design and postoperative rehabilitation technology, potentially reducing the risk of complications in the postoperative period.

Keywords: endoprosthesis; total hip replacement; complication; ceramics; brazing ceramics with titanium alloy; osseointegration



Citation: Popov, V.L.; Poliakov, A.M.; Pakhaliuk, V.I. Improving the Endoprosthesis Design and the Postoperative Therapy as a Means of Reducing Complications Risks after Total Hip Arthroplasty. *Lubricants* **2022**, *10*, 38. <https://doi.org/10.3390/lubricants10030038>

Received: 29 December 2021

Accepted: 28 February 2022

Published: 4 March 2022

Publisher's Note: MDPI stays neutral with regard to jurisdictional claims in published maps and institutional affiliations.



Copyright: © 2022 by the authors. Licensee MDPI, Basel, Switzerland. This article is an open access article distributed under the terms and conditions of the Creative Commons Attribution (CC BY) license (<https://creativecommons.org/licenses/by/4.0/>).

1. Introduction

Increasing the intensity and improving the quality of treatment of patients with injuries and diseases of the musculoskeletal system (MSS) are some of the primary problems of modern healthcare. This is due to the need to provide high-quality medical care to a large number of people, the number of which is increasing every year due to the increasing frequency of local military conflicts, changes in the structure of nutrition, physical activity, environmental conditions, as well as man-made and other factors. A relatively recent analysis of data on the global burden of disease (Global Burden of Disease, GBD) showed that approximately 1.71 billion people worldwide have MSS diseases, of which about 343 million people suffer from osteoarthritis [1].

Osteoarthritis is the most common form of joint damage and one of the main reasons leading to deterioration in the life quality of a large number of people [2]. The incidence of osteoarthritis increases sharply with age and is observed in more than half of people aged 65 and over, and in 80% of people aged 75 and over [3]. Very often, patients with joint osteoarthritis with severe pain that do not respond to conservative treatment, in the presence of serious joint dysfunction (before the development of significant deformities, joint instability, contractures and muscle atrophy), are recommended to replace the natural joint with an artificial one—an endoprosthesis [4,5]. Despite the critical nature and undesirability of this surgical operation (total hip arthroplasty, THA), it really is the only possible option in the prevailing conditions for the patient, allowing him to maintain the ability to lead an active lifestyle. In addition, it should be noted that currently THA is one of the most high-tech surgical operations, and the designs of joint endoprostheses and

their implantation technologies are constantly being improved, which in most cases makes it possible to achieve the desired result—to provide the patient with the highest possible quality of life.

Nevertheless, a joint endoprosthesis, as any implant, is a foreign body for the human body, and therefore the immune system in most cases triggers a defense response aimed at its rejection. Against the background of secondary immunodeficiency, usually formed as a result of a long-term degenerative-dystrophic process in the joint and surgical stress, the process of pathological osteolysis of periprosthetic bone tissue can be triggered, leading to a decrease in the strength of fixation of the implant in the bone. However, this is not the only reason that can lead to structural changes and, ultimately, to the destruction of the periprosthetic bone. This process is complex and is determined by a combination of demographic, constructive, surgical, rehabilitation and other factors. In other words, its initialization and course depend on age, gender, obesity, smoking, concomitant diseases, implant design, fixation method, therapeutic and rehabilitation strategies, etc. [6]. The destruction of the periprosthetic bone can lead to serious complications, including aseptic loosening, implant migration, and even a periprosthetic fracture and, as a result, the need for joint replacement—a technically more difficult, painful and expensive surgery.

For modular designs of total hip endoprostheses (total hip replacement, THR), another problem that reduces the reliability of THR is tribocorrosion [7]. Metal ions and wear particles released during tribocorrosion lead to undesirable consequences of both local and systemic nature [8]. In particular, they contribute to the appearance of pain, inflammation, edema, pseudotumors, genotoxicity [9], as well as the polarization of macrophages and accelerated corrosion by cells on the tapered interface of the stem with the endoprosthesis head [10,11]. In addition, biological fluids from the tissues surrounding the implant penetrate the interface of the modules and contribute to the formation of fretting corrosion [12–14]. In this regard, in recent years, a large number of publications have appeared, indicating an increase in the failure rate of modular THR associated with unfavorable local tissue responses [7,15].

The problems described above indicate that even well-studied and optimized designs of endoprostheses and joint replacement techniques, well-studied and optimized in relation to different quality criteria, still need to be improved. Modern trends in their improvement and development, formulated on the basis of an analysis of a large number of studies published in recent years, are presented in sufficient detail in [16]. This paper presents a new direction for improving the typical designs of modular hip replacements and postoperative rehabilitation strategies in order to reduce the risk of complications after THA.

2. Materials and Methods

2.1. Constructive and Technological Factors Influencing the Development of Complications after THR

THR is one of the most technologically advanced and successful surgical procedures consisting in replacing a natural hip joint with an artificial one, which in most cases leads to positive outcomes. However, serious complications associated with THR are also possible, which can be divided into three groups according to the timing of their occurrence:

- Intraoperative (fractures of the hip, pelvis, damage to the great vessels, perforation of the femoral canal);
- Early postoperative (suppuration, thrombosis, thrombophlebitis, dislocation of the endoprosthesis head, neuritis, decompensation of concomitant pathology);
- Late postoperative (deep suppuration, periprosthetic fractures, aseptic loosening, instability of implants due to improper planning of the operation or as a result of operation, destruction of the endoprosthesis components).

It is evident that constructive and technological factors are mainly determined by late postoperative complications, namely, aseptic loosening, instability, periprosthetic fractures and destruction of the endoprosthesis components [17]. In order to minimize

the influence of these particular factors on the development of complications after THR, the designs of endoprostheses and their implantation techniques are constantly being improved. When creating new designs, a systematic approach is used [18], taking into account their interaction with bone structures [19,20].

It should be noted that the main reason for THR failures (23%) is aseptic loosening against the background of periprosthetic osteolysis resulting from the activation of the innate immune response caused by the wear of the materials of the friction pairs [21]. The presence of wear debris in the periprosthetic tissue promotes the release of cytokines, which leads to inflammation and the activation of osteoclasts at the bone–implant interface and, ultimately, to the loosening and destruction of the implant. One of the main strategies to eliminate this problem to some extent, and thus to avoid revision THR, is to exclude or, at least, significantly reduce the wear of friction pair materials by increasing their wear resistance.

Currently, THR friction pairs are used:

- Polymers (polytetrafluoroethylene (PTFE), ultra-high molecular weight polyethylene (UHMWPE), cross-linked polyethylene (XLPE), highly cross-linked polyethylene (HXLPE), vitamin E-blended polymers, polyether-ether-ketone (PEEK), poly 2-methacryloyloxyethyl phosphorylcholine (PMPC), polycarbonate-urethane (PCU));
- Metals (Stainless steel, Cobalt-chromium-molybdenum (CoCrMo) alloys, Titanium alloys (Ti-6Al-4V), Zirconium alloy (Zr-2.5Nb));
- Metal alloy surface coatings (Titanium nitride (TiN), Silicon nitride (Si₃N₄), Diamond-like carbon (DLC), aluminum, nanocrystalline diamond (NCD));
- ceramics (aluminum ceramic, zirconia, zirconia-toughened alumina (ZTA), sapphire).

This is a fairly wide range of materials, which makes it possible to implement in THR many variants of two types of friction pairs [22]:

- hard-on-soft bearings (metal-on-polyethylene (MOP) is a metal femoral head and a polyethylene acetabular liner, ceramic-on-polyethylene (COP) is a ceramic femoral head and a polyethylene acetabular liner);
- hard-on-hard bearings (metal-on-metal (MOM), ceramic-on-ceramic (COC), and ceramic-on-metal (COM) is a ceramic femoral head and a metal acetabular liner).

The use of modern materials in friction pairs has made it possible to significantly improve the quality of THRs. However, the average lifespan of even such endoprostheses is currently 10–15 years. This period of time is too short for patients under 60 years of age, because the probable life expectancy of these people is about 20–25 years [23].

There is an opinion that one of the promising options for a THR friction pair is COP, despite its unpopularity in the surgical community due to its high cost, complexity, lack of study and propensity to catastrophic destruction [24,25]. Another disadvantage of this pair is the potential for the development of increased fretting and tribocorrosion in the area where the metal stem mates with the ceramic head. However, this is a complex problem inherent in all THRs with modular stems, depending, among other things, on the physiological state of the patient and the qualifications of the surgeon [26–31]. At the same time, modular stems have a significantly longer service life compared to single-piece ones, as well as such advantages as the ability to adjust the stem length and remove the head from the acetabulum during revision surgery [32,33]. This contradiction is one of the reasons why a universal solution to the problem of fretting and tribocorrosion has not yet been found [34].

The desire to reduce the risk of complications after THR has led to the development of implants with variable structure materials, including a continuous internal area covered with a porous surface layer [35–37]. The evident idea of this approach is that the strength of the implant is provided by the inner region, and the ingrowth of bone tissue into the porous surface layer leads to its reliable fixation in the bone. In general, this idea has found experimental confirmation, but the loosening of the endo-prostheses components

observed in some cases in the early postoperative period was an incentive to search for new endoprosthetic techniques.

For THR, along with materials of variable structure, it was proposed to use the cementless fixation of endoprostheses elements, which, according to the developers, should provide biocompatibility with body tissues, minimal bone remodeling, and stable primary and long-term biological fixation [38]. Recent data indicate excellent results of using THR with cementless fixation in the early postoperative period (at least two years after THA) [39]; similar results were obtained when analyzing the failure-free operation of the same THR for a long period of time (more than 18 years after THA) [40]. These and other facts contributed to the recognition of the cementless fixation technology, and now it has received significant development. It is believed that this technique served as the beginning of a new stage in the development of endoprosthetic technologies, the effectiveness of which is based, first of all, on the correspondence of the bone geometry, surface topology and the method of implant placement [41]. In addition, according to many THR specialists, cementless fixation helps to reduce the risk of loosening of the THR components in the postoperative period.

The efficiency of cementless fixation can be significantly increased so that the best conditions for early osseointegration of implants are provided. To a certain extent, this can be achieved by improving the structures of THR in order to achieve the desired morphological, physicochemical, and biochemical properties of the surfaces of their elements, which are interfaced with bone tissue. Currently, most of the research in this area is focused on the study of the mechanical state of the bone after implant placement on the basis of phenomenological models of osseointegration or bone remodeling [42,43]. The study of such models allows to some extent to evaluate the influence of the geometry of the implant and the topography of the surface of its elements on the quality of THR. However, they do not fully take into account the biological processes occurring in the bone tissue and, therefore, they do not allow for the evaluation of the effect of the implant on the development of these processes. More reliable information can be obtained in the study of mechanobiological models describing biological processes occurring in the periprosthetic bone tissue together with the processes of changes in its structure and mechanical properties [44].

2.2. Mechanobiological Models of Implant Osseointegration

The healing of periprosthetic bone after THR, as the healing of bone fractures, occurs as a result of a cascade of complex biological events. In the modern interpretation, these events are described quite informatively in [45]. It is known that various molecules take part in them, which can be divided into three groups: (1) pro-inflammatory cytokines; (2) growth factors; and (3) metalloproteinases and angiogenic factors [46,47]. It is also known that biochemical processes leading to the healing of bone tissue occur in a certain spatial environment and in a certain time sequence [48]. If we take into account the essence of THR, then these facts are enough to formulate various hypotheses and build mathematical models of these processes [49].

The mandatory procedure for THR is the resection of the femoral head and preparation of the stem bed in the femur. It is accompanied by surgical trauma and damage to the blood vessels, which leads to the filling of the cavity formed in the bone with blood. After the installation of the implant, proteins from the blood and tissue fluid are adsorbed on its surface; platelets are activated, releasing adhesion molecules, lipids and growth factors, which, in turn, regulate the function of keratinocytes, as well as the processes of migration and proliferation of fibroblasts and endothelial cells [50–52]. It is known that an increase in the micro texture of the implant surface with the corresponding surface roughness promotes the adhesion and activation of platelets and, as a consequence, accelerates the healing and osseointegration processes [53,54].

After the implantation of the endoprosthesis, due to an extraordinary situation for the body, the homeostasis system is activated and a fibrin network begins to form in the periprosthetic space. A localized decrease in blood circulation causes cell necrosis and the immune system triggers an inflammatory response. Neutrophils and macrophages,

under the influence of chemical stimuli along the chemotaxis gradient, reach damage and remove necrotic cells from the tissue. In parallel with this, the process of angiogenesis is triggered, as a result of which a new vascular network is formed in the bone surrounding the implant [55,56]. As a result, osteogenic cells are able to migrate from the surface of the periprosthetic bone to the surface of the implant and differentiate into osteoblasts, which ultimately lead to the formation of a bone matrix. The development of this process depends on the mechanical state of the tissue and its changes and is regulated by growth factors [57]. It has been established that mechanical loading can lead to an increase in the secretion of growth factors, which, in turn, promotes the differentiation of osteogenic cells into osteoblasts and osseointegration of the implant [58,59]. At the moment, it is known that implants exposed to functional loading demonstrate a higher degree of contact with the bone than unloaded implants at an early stage of the postoperative period [60]. In this case, the stresses arising in the bone tissue during mechanical loading, contribute to an increase in the volume and density of bone tissue [61]. However, in the process of adaptation of bone tissue to mechanical stress, its resorption can occur [62], despite the fact that mechanical loading does not significantly affect the activation of osteoclasts in the periprosthetic bone [63].

A more detailed description of the biochemical processes occurring in the bone tissue after the implantation into it can be found in [64–67]. However, for the development of practically significant strategies for accelerated healing of periprosthetic tissues and osseointegration of implants after THR, it may be sufficient to study simplified models, since refined multifactorial models of most natural processes, including biochemical ones, as a rule, do not allow achieving the expected effect [68]. First of all, this is explained by the fact that the refinement of the mathematical model, which usually leads to its complication, simultaneously requires the refinement of the parameters included in it, which, as noted above, are very variable under THR conditions and depend on many uncontrollable factors. However, it is obvious that in all mathematical models that can potentially be used to study the processes of implants osseointegration, the results of numerous experimental studies should be taken into account, as, for example, in the model of A. Bailón-Plaza and M. van der Meulen, developed for the *in silico* research of the healing of bone fractures [69]. In this model, the migration of osteogenic cells is described considering their random dispersion, established experimentally, under the condition of contact inhibition. Cell proliferation is modeled considering the diffusion of nutrients and the conditions of logistic growth, in which the rate of cell division decreases linearly with an increase in their density and, as a consequence, with space limitation. In this case, the size of a stable cell population corresponds to the experimentally established maximum density at which cell death as a result of apoptosis is balanced by the mitosis of new cells. The experimentally confirmed enhancing and inhibiting effects of the extracellular matrix at its low and high density, respectively, are also taken into account. The system of equations of such a model in dimensionless form is represented as follows [69,70]:

$$\frac{\partial c_m}{\partial t} = \nabla \cdot [D_{cm} \nabla c_m - C_{cm} c_m \nabla m] + A_m c_m [1 - \alpha_m c_m] - F_1 c_m - F_2 c_m \quad (1)$$

$$\frac{\partial c_c}{\partial t} = A_c c_c [1 - \alpha_c c_c] + F_2 c_m - F_3 c_c \quad (2)$$

$$\frac{\partial c_b}{\partial t} = A_b c_b [1 - \alpha_b c_b] + F_1 c_m + F_3 c_c - d_b c_b \quad (3)$$

$$\frac{\partial m_c}{\partial t} = P_{cs} (1 - k_c m_c) (c_m + c_c) - Q_{cd2} m_c c_b \quad (4)$$

$$\frac{\partial m_b}{\partial t} = P_{bs} (1 - k_b m_b) c_b \quad (5)$$

$$\frac{\partial g_c}{\partial t} = \nabla \cdot [D_{gc} \nabla g_c] + E_{gc} c_c - d_{gc} g_c \quad (6)$$

$$\frac{\partial g_b}{\partial t} = \nabla \cdot [D_{gb} \nabla g_b] + E_{gb} c_b - d_{gb} g_b \quad (7)$$

where $\nabla (*) = grad (*)$ is the gradient of the scalar function (*), $\nabla \cdot [\nabla (*)] = div [grad (*)] = \nabla^2 (*)$ is the divergence $grad (*)$; c_m, c_c, c_b are the current concentrations, $K_{lm} = \frac{1}{\alpha_m}$, $K_{lc} = \frac{1}{\alpha_c}$, $K_{lb} = \frac{1}{\alpha_b}$ are the limiting concentrations, A_m, A_c, A_b are the degrees of mesenchymal cells, chondrocytes and osteoblasts proliferation, respectively; m_c, m_b, g_c, g_b are the matrix volumetric densities of the connective/cartilage tissue, bone tissue, chondrogenic and osteogenic growth factors, respectively; D_{cm}, C_{cm} are haptotactic and haptokinetic rates of cell migration; F_1, F_2, F_3 are functions that link cell differentiation with the concentration of growth factors; P_{cs}, P_{bs} are constants representing connective/cartilage and bone matrix; Q_{cd1}, Q_{cd2}, Q_{bd} are constants representing matrix degradation; D_{gc}, D_{gb} are the diffusion coefficients of chondrocytes and osteoblasts; E_{gc}, E_{gb} are functions that link the production of growth factors with the concentration of growth factors; d_{gc}, d_{gb} are decay constants. Sets of calculated model parameters:

$$B_m = \frac{A_m}{K_{lm}} = \alpha_m A_m, B_c = \frac{A_c}{K_{lc}} = \alpha_c A_c, B_b = \frac{A_b}{K_{lb}} = \alpha_b A_b, Q_{cd1} = k_c P_{cs}, Q_{bd} = k_b P_{bs} \quad (8)$$

$$D_{cm} = \frac{D_h}{K_h^2 + m^2} m, C_{cm} = \frac{C_k}{(K_k + m)^2} \quad (9)$$

$$A_m = \frac{A_{m0}}{K_m^2 + m^2} m, A_c = \frac{A_{c0}}{(K_c + m)^2} m, A_b = \frac{A_{b0}}{(K_b + m)^2} m \quad (10)$$

$$F_1 = \frac{Y_1}{H_1 + g_b} g_b, F_2 = \frac{Y_2}{H_2 + g_c} g_c, F_3 = \frac{m^6}{B_{c0}^6 + m^6} \cdot \frac{Y_3}{H_3 + g_b} g_b \quad (11)$$

$$E_{gc} = \frac{G_{gc} g_c}{H_{gc} + g_c} \cdot \frac{m}{K_{gc}^3 + m^3}, E_{gb} = \frac{G_{gb} g_b}{H_{gb} + g_b} \quad (12)$$

It should be noted that the Equations (1)–(7) was used to study the processes of fracture healing in various versions. However, in the context of this work, its modification was of interest to study the processes of healing the periprosthetic tissues and osseointegration of implants. For example, the model used by P. Moreo and colleagues to study the process of osseointegration of dental implants can be considered quite plausible and suitable for these purposes [71]. In mathematical form, it is represented as a system of eight partial differential equations:

$$\frac{\partial T}{\partial t} = \nabla \cdot [D_T \nabla T - H_T T \nabla p] - A_T T \quad (13)$$

$$\frac{\partial C}{\partial t} = \nabla \cdot [D_C \nabla C - (K_1 \nabla f_1 + K_2 \nabla f_2) C] + \left(\alpha_{C0} + \frac{\alpha_C f_1}{\beta_C + f_1} + \frac{\alpha_C f_2}{\beta_C + f_2} \right) \left(1 - \frac{C}{N} \right) C - \frac{\alpha_{CB} f_1}{\beta_{CB} + f_1} C - A_C C \quad (14)$$

$$\frac{\partial B}{\partial t} = \frac{\alpha_{CB} f_1}{\beta_{CB} + f_1} C - A_B B \quad (15)$$

$$\frac{\partial f_1}{\partial t} = \nabla \cdot [D_{f1} \nabla f_1] + \left(\frac{\alpha_{T1} p}{\beta_{T1} + p} + \frac{\alpha_{T2} f_1}{\beta_{T2} + f_1} \right) T - A_{f1} f_1 \quad (16)$$

$$\frac{\partial f_2}{\partial t} = \nabla \cdot [D_{f2} \nabla f_2] + \frac{\alpha_{C2} f_2}{\beta_{C2} + f_2} C + \frac{\alpha_{B2} f_2}{\beta_{B2} + f_2} B - A_{f2} f_2 \quad (17)$$

$$\frac{\partial v_f}{\partial t} = \frac{-\alpha_w f_2}{\beta_w + f_2} (1 - v_w) v_f B \quad (18)$$

$$\frac{\partial v_w}{\partial t} = \frac{\alpha_w f_2}{\beta_w + f_2} (1 - v_w) v_f B - \gamma (1 - v_l) v_w \quad (19)$$

$$\frac{\partial v_l}{\partial t} = \gamma (1 - v_l) v_w \quad (20)$$

A description of the state variables, parameters and coefficients of the model, as well as their numerical values, is given in Appendix A. Subsequently, these parameter values were taken as estimates for modeling the processes of implant osseointegration.

An important advantage of the Equations (13)–(20) are the ability to consider the effect of the implant surface roughness on the osseointegration process. In addition, it can be adapted to assess the effect on osseointegration of artificial extracellular matrices implanted in the periprosthetic space, cell therapy, and stimuli of various natures. At the same time, results that are important for practice can be obtained by studying even simpler models. For example, the following simplified models were proposed in [72]:

Model (1):

$$\frac{\partial C}{\partial t} = \nabla \cdot [D_C \nabla C - CK_2 \nabla f_2] + g(C, f_2, B) \quad (21)$$

$$\frac{\partial f_2}{\partial t} = \nabla \cdot [D_{f_2} \nabla f_2] + g_{f_2}(C, f_2, B) \quad (22)$$

$$\frac{\partial B}{\partial t} = g_{CB}(C, f_2, B) \quad (23)$$

where $g_C(C, f_2, B) = \sigma \left(1 + \frac{\alpha_C f_2}{\beta_C + f_2}\right) C(1 - C) - (\alpha_{CB} + A_C)C$, $g_{f_2}(C, f_2, B) = \frac{\alpha_2 f_2}{\beta_2 + f_2} (C + B) - A_{f_2} f_2$, $g_{CB}(C, f_2, B) = \alpha_{CB}C - A_B B$, $\alpha_{C2} = \alpha_{B2} = \alpha_2$, $\beta_{C2} = \beta_{B2} = \beta_2$;

The model (2):

$$\frac{\partial C}{\partial t} = D_C \nabla^2 C + \sigma C(1 - C) - (\alpha_{CB} + A_C)C \quad (24)$$

$$\frac{\partial B}{\partial t} = \alpha_{CB}C - A_B B \quad (25)$$

$$\frac{\partial v_f}{\partial t} = -\alpha_w(1 - v_w)v_f B \quad (26)$$

$$\frac{\partial v_w}{\partial t} = \alpha_w(1 - v_w)v_f B - \gamma(1 - v_l)v_w \quad (27)$$

$$\frac{\partial v_l}{\partial t} = \gamma(1 - v_l)v_w \quad (28)$$

In Equations (21)–(23), in contrast to Equations (13)–(20), it is assumed that the stimulating effect of growth factors of type 2 on the secretion of osteogenic cells and osteoblasts is the same, and the absence of platelets and growth factors of type 1 in it does not allow assessing the effect of microrelief the implant surface for osteogenesis. The Equations (24)–(28) does not directly consider the influence of platelets and growth factors on the osseous integration of the implant. However, these factors are indirectly taken into account by the inclusion of osteogenic cells and osteoblasts, which allows an approximate assessment of the dynamics of osseointegration [72].

Considering the foregoing, a research plan was developed, shown in Figure 1 in the form of a scheme, on the ways to achieve the goals of this work, which are highlighted in green. At the same time, the THR is considered as a certain heterogeneous system, whose elements are synergistically related to each other [18]. Therefore, the synthesis of THR should be carried out taking into account many restrictions, conditions and criteria, which may be contradictory. In such cases, it would be ideal for the problem to build a Pareto-optimal set of solutions, the best of which can be determined either by a subjective method of expert assessments, or in the process of long-term operation of various THR designs. At the same time, some possible solutions with a high probability can be considered to meet all the THR quality criteria, even in cases where they only to a certain extent allow us to get closer to the goal. In this case, these are solutions that allow reducing fretting and tribocorrosion in the area where the metal stem meets the ceramic head, as well as intensifying the processes of implant osseointegration in the early postoperative period.

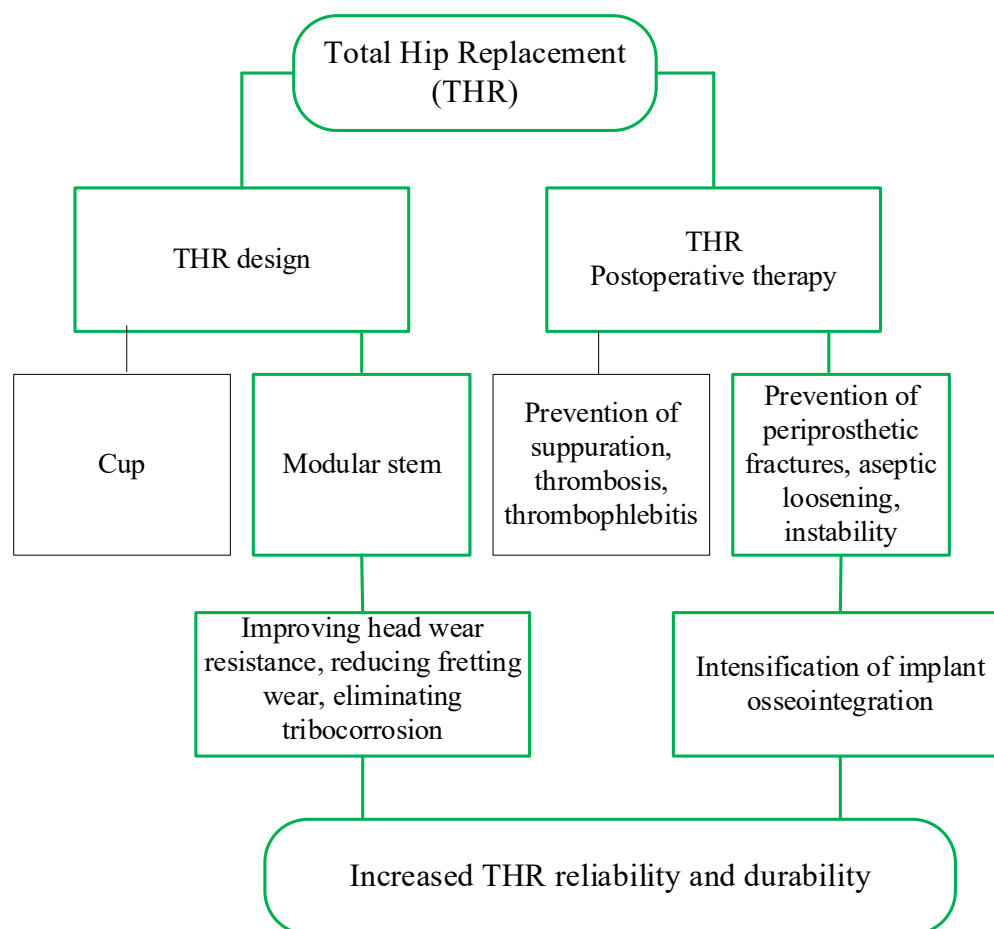


Figure 1. Scheme of the study.

3. Results and Discussion

Taking into account the current level of technology and technical means of THA, the improvement of this surgical procedure, in addition to the direct improvement of the surgical technique, must necessarily include the elimination of the structural defects of implants and the improvement of postoperative rehabilitation strategies. At the same time, as noted above, an important role should be assigned to eliminating the causes of osteolysis and loosening of implants.

To reduce material wear, which is most conducive to the development of osteolysis, it is advisable to use well-proven ceramics-on-polyethylene (CoP) friction pairs in THR, provided that the disadvantages inherent in the ceramic heads are eliminated, such as the tendency to brittle fracture, increased fretting and tribocorrosion in the interface with metal stem. One approach to eliminate these disadvantages is to ensure that there is no moving contact between dissimilar materials and to reduce the likelihood of tensile stresses in the brittle head. To solve this problem, an extensive analysis of the current state of the art was performed, which can be briefly summarized as follows.

The known THR designs couple the ceramic head with the stem neck and are used adapter sleeves. Among them, there are plastic sleeves [73], whose disadvantage is that they cannot provide reliable fixation of the stem neck and head from the relative axial movements that occur during the operation of the prosthesis due to their soft properties. This contributes to the violation of the joint biomechanics and the occurrence of a probable pain syndrome, which, ultimately, can lead to joint revision prosthetics. There are also THR designs, in which the taper interfaces of the titanium alloy adapter metal sleeve are made, both with the head and with the stem neck [74]. However, in [75], it was shown that, during the prosthesis operation, there are micro displacements of the sleeve, both

rotational and translational, in the opening of the head and on the stem neck. Therefore, this phenomenon does not exclude the possibility of ceramic destruction when the prosthesis is exposed to extreme dynamic loads due to the presence of a movable taper junction between the head and the sleeve, which, thereby, also contributes to the occurrence of fretting corrosion and the release of its products into the surrounding tissues. The design of THR is also known as a patent for an invention [76], where, in order to exclude the mobility of the junction between the head and the metal sleeve, it was proposed to connect them by low temperature soldering where the head is made of single crystal sapphire or ruby. The disadvantage is that, in the available literature, the soldering of ceramics at low temperature with biocompatible solders is practically not found and is probably hardly possible, because only active metals can “wet” ceramics and among them only three are biocompatible, titanium, zirconium and hafnium, and, as it is known, solders based on titanium, zirconium and hafnium are high temperature. In this case, when applying brazing (high temperature) for anisotropic single crystals of sapphire or ruby to a metal sleeve having different temperature coefficients of linear expansion, there is a high probability of cracks being formed in the ceramics, which is unacceptable in products of this type. Given this analysis, an improved design of the ceramic head and its manufacturing technology was developed. A general view of an experimental sample of this head, made for tensile testing, and its internal structure is shown in Figure 2.

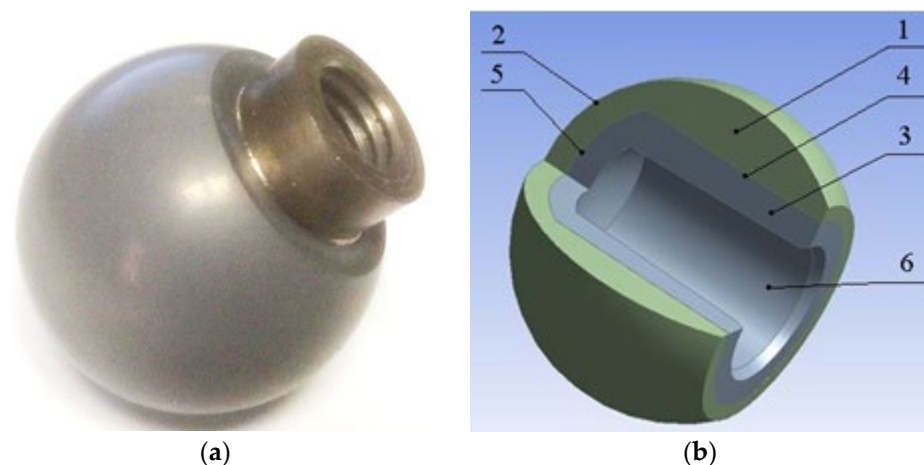


Figure 2. The improved ceramic head: (a) general view of the experimental sample; (b) elements of the internal structure (description of elements indicated by numbers is given in the text below).

The head consists of an external ceramic element 1 with a spherical outer surface 2 and an inner blind hole in which a metal sleeve 3 is placed. The sleeve is limited by an outer cylindrical surface 4, ending with an end piece 5 and an inner blind axial taper surface 6. Ceramic head element 1 and a sleeve 3 are bonded by brazing, which ensures high strength of the joint and eliminates moving contact between dissimilar materials during operation. When assembling a metal stem with a head, its taper element mates with the corresponding conical surface 6 of the sleeve.

A titanium alloy, for example, BT1-0 or Ti-6Al-4V, is used as a metal element (sleeve), and alumina or zirconia ceramics are used as a ceramic element. The performed finite element analysis of the head design with no sleeve showed that the greatest stresses and strains in the ceramics were at the outlet in the head. In the presence of a sleeve, the zone with maximum stresses and strains shifted to the area where the ceramics are practically the thickest, and the values of stresses and strains reduced by more than 2 times [77], on the basis of which the thicknesses of the sleeve and ceramics 1 were selected, also considering the requirements of medical standards. To create a fixed joint between the ceramic element of the head and the titanium alloy sleeve, the technology of their brazing was developed, as well as the solder itself with the required biocompatibility index [78].

This head design combines all the advantages of both metal and ceramic heads. In it, the presence of a metal sleeve with a traditionally taper axial hole provides a fixed joint of the ceramic head with the sleeve due to the absence of micro-movements along the outer sleeve surface, thereby protecting the head from possible splitting in the taper connection, which significantly increases the stability of the THR. Thus, this head also improves the reliability and durability of the THR by reducing wear in the COP friction pair by eliminating fretting corrosion in the brazed joint, which has a significant impact on the development of the periprosthetic bone tissue osteolysis.

Another challenge to improve the reliability of THR is to provide the accelerated osseointegration of the implant. Its solution requires considering many factors that influence the course of this process. It was shown above that the best conditions for osseointegration are achieved with the cementless fixation of implants with a developed surface microrelief. This helps to increase the adsorption of proteins on the surface and the activation of platelets. Experimental data indicate that the concentration of platelets reaches the highest value on the surface of the implant and very quickly decreases with distance from it. In addition, it is known that the density of chondrocytes increases with an increase in the surface microrelief. With a sufficient accuracy for approximate models, the platelet population density at a point in space located at a distance x from the implant surface can be described by the dependence:

$$p(x) = p_{k0} \cdot e^{-qx}, \quad (29)$$

where $p_{k0} = const$ is a constant, depending on the nature of the microrelief; and $q = const$ is an indicator of the rate decrease in density.

Considering that the dynamics of platelet density changes described by Equation (13) does not depend on changes in other variables of the state of Equations (13)–(20), it can be studied independently of these variables.

The solutions of Equation (13) with the initial conditions $T_1(x, 0) = p_{10} \cdot e^{-2x}$ and $T_2(x, 0) = p_{20} \cdot e^{-2x}$, where $p_{10} = 0.1 \frac{mg}{mm^2}$ and $p_{20} = 0.5 \frac{mg}{mm^2}$ in dimensionless form were obtained in MATLAB and are shown graphically in Figure 3. Their analysis confirms the adequacy of the Equations (13)–(20), since the obtained dependences correspond to the experimental data. That is, the platelet population is grouped in the vicinity of the implant surface and rapidly decreases with distance from it. Nevertheless, platelet activation after THR triggers a cascade of biological events important for the healing of periprosthetic tissues, including the release of adhesion molecules that provide the movement of leukocytes to the inflammation area, lipids that affect cell permeability and the activity of many enzymes and growth factors that stimulate the proliferation and differentiation of fibroblasts, and endothelial cells. Evidently, an increase in the initial platelet density corresponds to an increase in biological processes, and, therefore, an increase in the surface microrelief contributes to a better osseointegration of the implant.

The osseointegration process consists of the formation of mature bone tissue on the implant surface, which is integrated with the host bone. For its initialization, it is necessary to provide a sequence of biological events that ensure the formation of a collagen matrix in the periprosthetic space. To analyze them, we used the simplified Equations (21)–(23) and Equations (24)–(28).

In [72] it was shown that the expressions $g_C(C, f_2, B)$, $g_{f2}(C, f_2, B)$, and $g_{CB}(C, f_2, B)$, depending on the values of the model parameters, determine the course of the osseointegration process, which is determined depending on the mode parameter $\chi = \alpha_{C2} \left(1 + \frac{\alpha_{CB}}{A_B}\right)$, including stable and unstable modes, as well as bifurcation zones. In this regard, a comparative analysis of the nature of the change in the state variables of the Equations (13)–(15) depending on the value of χ was carried out. The study of the model equations in dimensionless form was carried out in the MATLAB environment by the finite element method using the pde function. In Figures 4 and 5, the processes of changes in the concentration of osteogenic cells and osteoblasts are shown, respectively, at $\chi = 2.8; 3.0; 7.5; 10$.

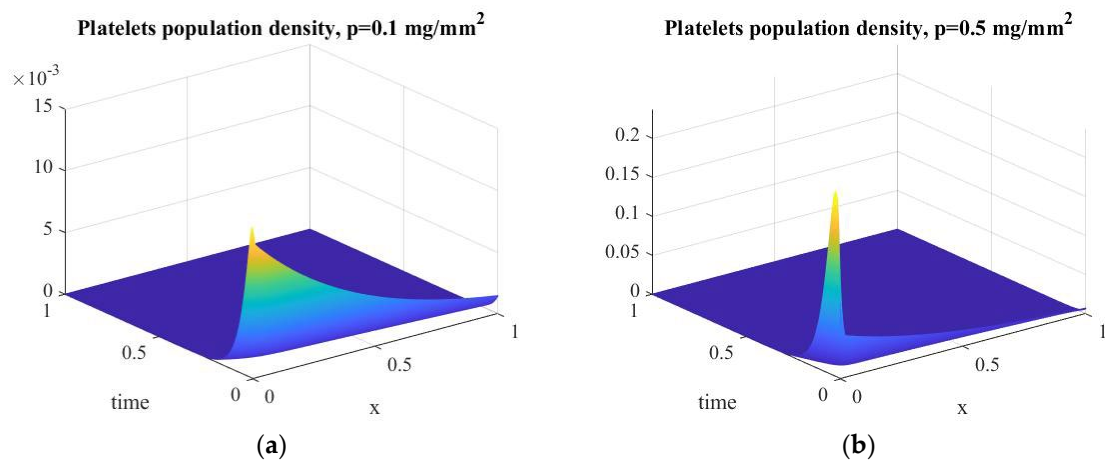


Figure 3. Change in platelet population density: (a) $p(x) = p_{10} \cdot e^{-2x}$; (b) $p(x) = p_{20} \cdot e^{-2x}$.

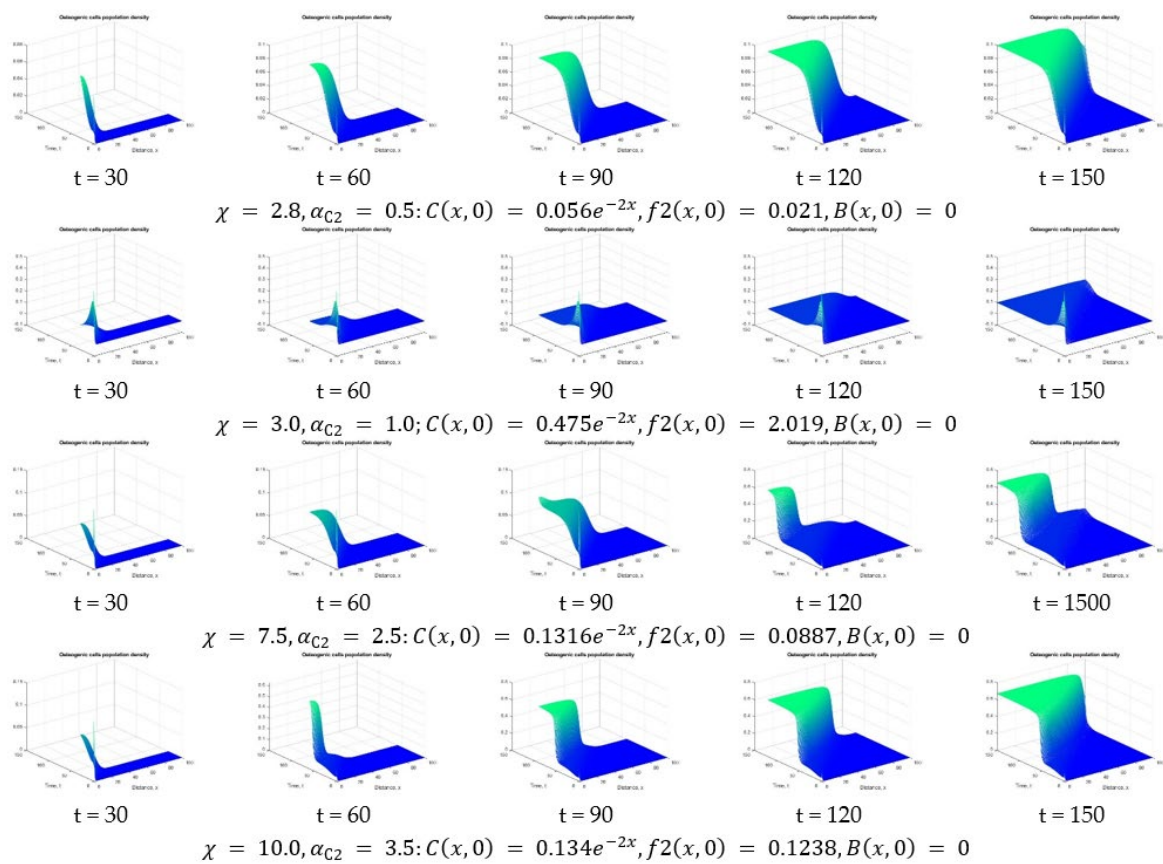


Figure 4. Dynamics of the processes of changes in the concentration of osteogenic cells in the periprosthetic space under different modes of implant osseointegration.

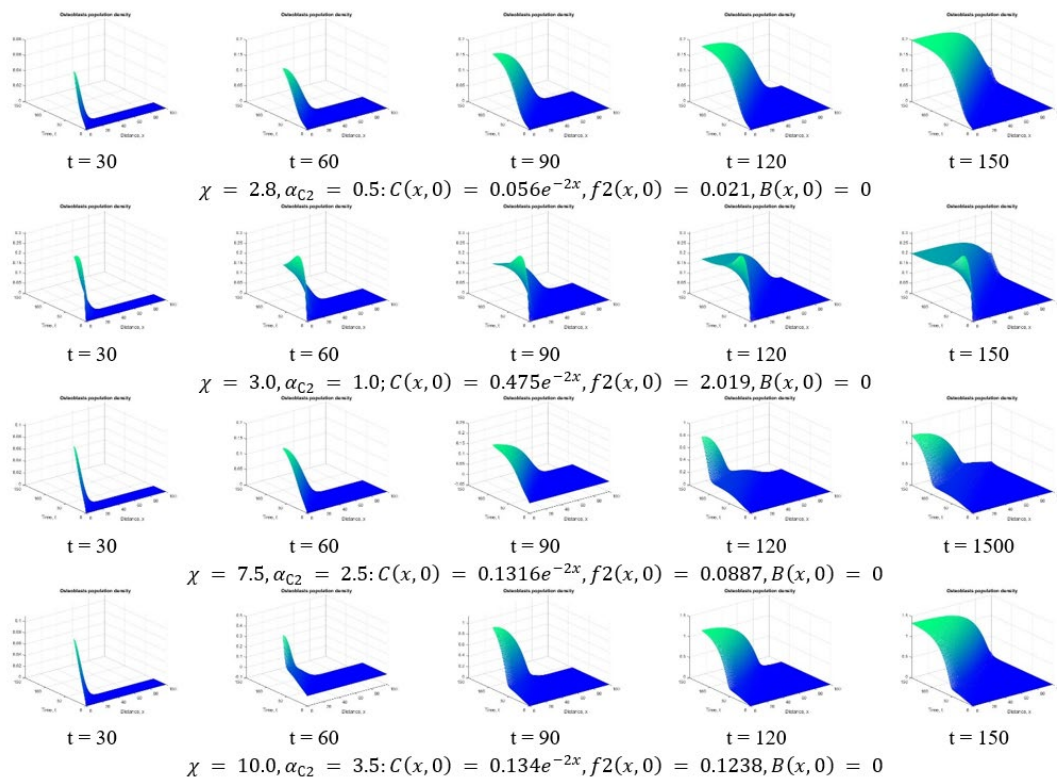


Figure 5. Dynamics of the processes of changes in the concentration of osteoblasts in the periprosthetic space under different modes of implant osseointegration.

It is easy to see that the change in the cellular environment of the implant significantly depends on the mode of osseointegration and under different modes, characterized by the corresponding value of the coefficient of natural secretion of growth factors of type 2 in the environment of osteogenic cells (α_{C2}), which occurs in different ways. Considering this result, the issue of ensuring the desired mode of osseointegration, determined, inter alia, by the value of α_{C2} , becomes relevant.

From Equation (24) it follows that the decrease in the density of osteogenic cells is influenced by their natural death, determined by the coefficient A_C and growth factors of type 1, increasing the proliferation of osteoblasts, determined by the coefficient α_C . In this regard, the nature of the processes of osseointegration depends on the total influence these factors, i.e., from the value of $\alpha_{C2} + A_C$. The numerical solutions of the equations of the Equations (24)–(28) in dimensionless form depending on the value of $\alpha_{C2} + A_C$ were obtained at constant values of the osseointegration mode $\chi = 3.0$ and the coefficient of the natural secretion of growth factors of type 2 in the environment of osteogenic cells $\alpha_{C2} = 1.0$, zero conditions at the boundaries and initial conditions, taking into account the change in osteogenic cells in the periprosthetic space at the initial moment of time. These solutions are shown graphically in Figure 6.

Finally, in order to elucidate the influence of one of the significant parameters of the Equations (24)–(28), namely, the diffusion coefficient of osteogenic cells D_C , on the nature of osseointegration, the numerical solutions of Equations (24)–(28) were obtained in dimensionless form, shown in Figures 6 and 7 depending on the D_C at constant values $\chi = 7.5, \alpha_{C2} = 2.5, \alpha_{CB} + A_C = 1.35$, zero conditions at the boundaries and initial conditions, considering the change in osteogenic cells in the periprosthetic space at the initial time.

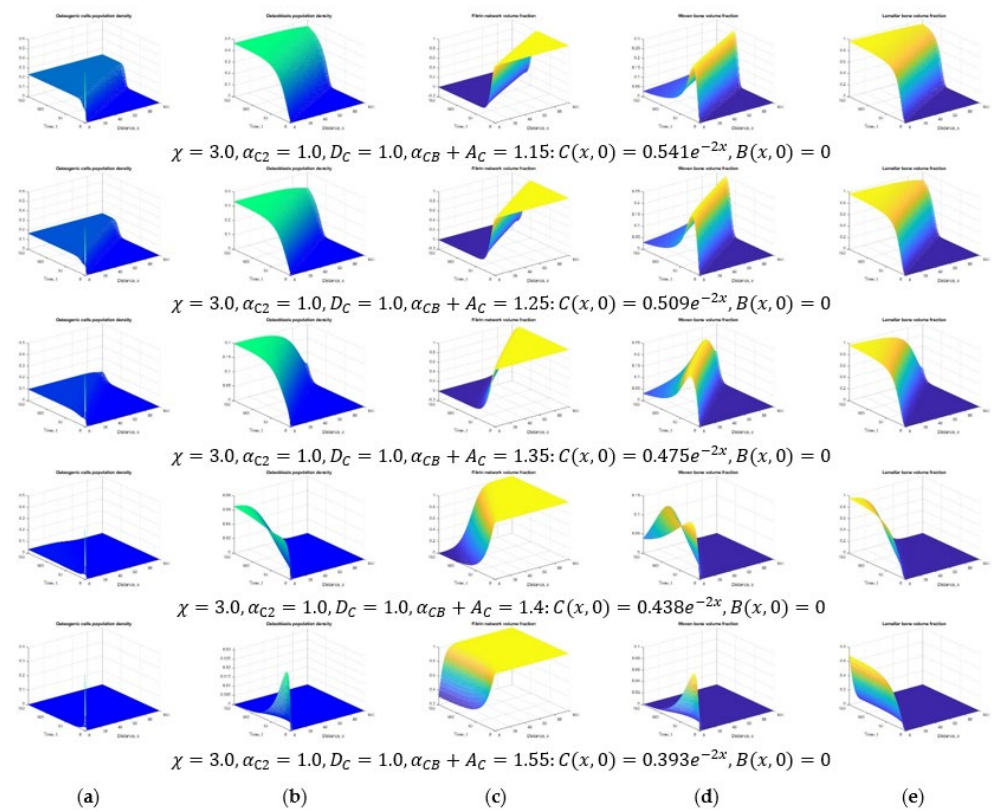


Figure 6. Changes in the state variables of the Equations (24)–(28) depending on the parameters that determine the natural death of osteogenic cells and the influence of type 1 growth factors on the proliferation of osteoblasts: (a) Osteogenic cells population density; (b) Osteoblasts population density; (c) Fibrin network volume fraction; (d) Woven bone volume fraction; (e) Lamellar bone volume fraction.

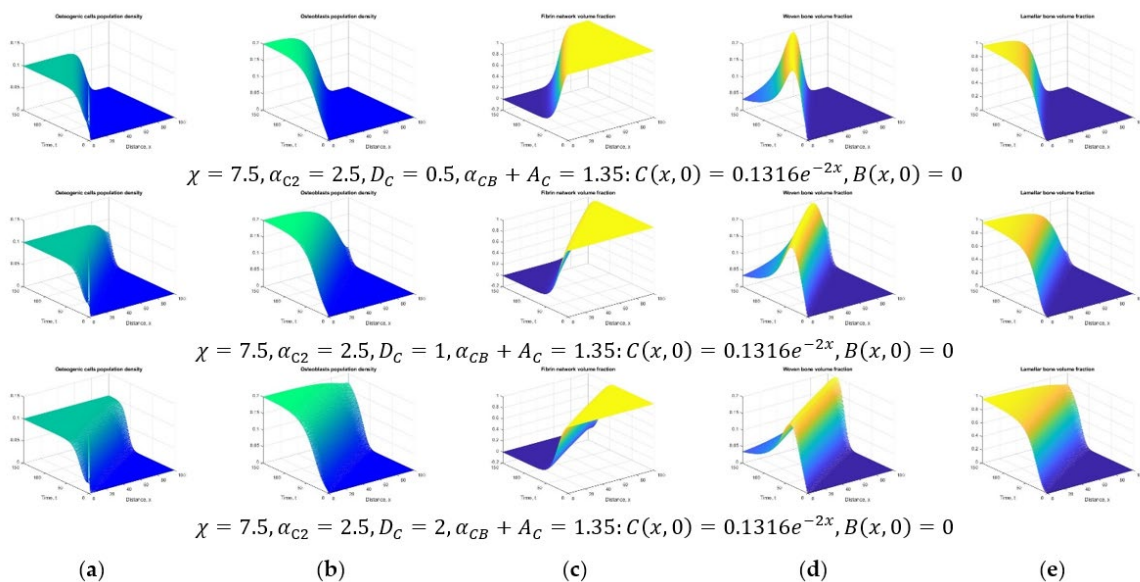


Figure 7. Change in the state variables of the Equations (24)–(28) depending on the diffusion coefficient of osteogenic cells: (a) Osteogenic cells population density; (b) Osteoblasts population density; (c) Fibrin network volume fraction; (d) Woven bone volume fraction; (e) Lamellar bone volume fraction.

An elementary analysis of the presented family of graphs indicates that the value of the diffusion coefficient of osteogenic cells also has a noticeable effect on the course of osseointegration. A decrease in D_C leads to a reduction in the area of new bone tissue formation, and vice versa. It can be assumed that with the help of certain therapeutic procedures it is possible to achieve such a state of the periprosthetic tissues in which the best conditions for early osseointegration of the implant will be achieved.

4. Conclusions

The main goal of this study was to substantiate one of the possible approaches to reduce the risks of complications in the late postoperative period and, thereby, to increase the durability of THR. At the modern technological level, this can be achieved by eliminating the obvious shortcomings of THR designs and using postoperative therapeutic procedures that ensure reliable osseointegration of the implant immediately after its implantation.

On the face of it, the proposed head improvement of the modular stem would have little effect on THR durability. However, in reality, this improvement can significantly improve the reliability of the implant as a whole. Firstly, such a head has all the significant advantages in a CoP type pair, but, along with minimal wear of the pair materials, it is also characterized by the high strength inherent in metal-on-polyethylene (MoP) pairs. Secondly, the elimination of relative micromovements between THR elements made of dissimilar materials significantly reduces fretting and tribocorrosion, thus eliminating the main problem of a CoP pair, which is a high probability of osteolysis in bone tissue, caused by the appearance of many tiny wear particles. Consequently, the likelihood of the risk of postoperative complications leading to the need for early revision THR with such a head is significantly reduced.

However, late postoperative complications can also occur due to the loosening of the implant, which can occur for a number of objective and subjective reasons. Most often, as shown above, this is due to the poor osseointegration of the implant. The results of the numerical analysis performed in this study confirm the experimental data indicating that the course of osseointegration processes depends on many factors of both mechanical and biological nature. An important role in this is played by the type of periprosthetic bone tissue into which the implant is installed: spongy or cortical. It is clear that cortical tissue has significantly greater strength than spongy tissue, but it contains a much smaller number of osteogenic cells that can be involved in the process of osseointegration. Therefore, the formation of the bone matrix in the periprosthetic space should proceed better in the spongy tissue than in the cortical tissue. However, the placement of an implant in a space surrounded by spongy tissue is undesirable due to its low mechanical properties. In this regard, possible early postoperative therapy can be aimed at a temporary decrease in the density of periprosthetic cortical tissue in order to intensify the biological processes of osseointegration. At the same time, as the results of numerical modeling performed in this study show, the diffusion coefficient D_C changes, which has a significant effect on the nature of the osseointegration process.

In addition, to ensure the best conditions for osseointegration, it is necessary to choose the optimal mode characterized by the parameter χ , which, in turn, is determined by the coefficient of influence of growth factors of type 1 on the proliferation of osteoblasts α_{CB} and the coefficient of natural secretion of growth factors of type 2 in the environment of osteogenic cells α_{C2} . It is known that a low-amplitude periodic load acting on damaged tissues has a stimulating effect on the differentiation of osteogenic cells [79,80] and the secretion of growth factor type 2 [81,82]. Therefore, the mode of osseointegration χ can be considered as a parameter that determines the intensity of the mechanical stimulation of osteogenic cells. However, at the same time, in [72], it is considered as some generalized parameter of stimulation, without specifying the nature of physical stimuli. Thus, for the best osseointegration of the implant in the early postoperative period, it is desirable to use rehabilitation procedures, including, for example, the low-amplitude high-frequency stimulation of periprosthetic tissues. Moreover, the stimulation parameters must be strictly

individualized and take into account the biomechanical and biochemical state of a particular patient. In mathematical models, these states are reflected in the form of model parameters, which, as shown by the simulation results, have a significant impact on the nature of osseointegration.

It should also be noted that the mechanical stimulation of tissues damaged by a THR can lead to a better effect if artificial biodegradable extracellular matrices are placed in the periprosthetic space. This procedure can currently be performed by injection. As a result, more osteoblasts will be recruited for the formation of new bone matrix, which, in turn, will potentially contribute to an increase in the rate of implant osseointegration and an increase in the reliability of a THR.

Author Contributions: Conceptualization, A.M.P.; investigation, V.L.P. and V.I.P.; software, A.M.P.; writing—original draft preparation, A.M.P.; writing—review and editing, V.L.P. and V.I.P. All authors have read and agreed to the published version of the manuscript.

Funding: This research received no external funding.

Data Availability Statement: Data are contained within the article.

Acknowledgments: The authors acknowledge a G.D. Olinichenko, for his helpful comments in preparing this paper. The authors acknowledge support by the Open Access Publication Fund of TU Berlin.

Conflicts of Interest: The authors declare no conflict of interest.

Appendix A

Table A1. Nomenclature *.

Model state variables			
Platelets population density	T		$\text{cells}\cdot\text{mL}^{-1}$
Osteogenic cells population density	C		$\text{cells}\cdot\text{mL}^{-1}$
Osteoblasts population density	B		$\text{cells}\cdot\text{mL}^{-1}$
Type 1 growth factors concentration (PDGF, TGF- β)	f_1		$\text{ng}\cdot\text{mL}^{-1}$
Type 2 growth factors concentration (BMP, superfamily TGF- β)	f_2		$\text{ng}\cdot\text{mL}^{-1}$
Fibrin network volume fraction	v_f		mL^{-1}
Woven bone volume fraction	v_w		mL^{-1}
Lamellar bone volume fraction)	v_l		mL^{-1}
Concentration of adsorbed proteins (принимается в зависимости от состояния поверхности имплантата)	p	-	$\mu\text{g}\cdot\text{mm}^{-2}$
Constant model parameters			
Platelet diffusion coefficient	D_T	1.365×10^{-2}	$\text{mm}^2\cdot\text{day}^{-1}$
Diffusion coefficient of osteogenic cells	D_C	0.133	$\text{mm}^2\cdot\text{day}^{-1}$
Diffusion coefficient of type 1 growth factors	D_{f1}	0.3	$\text{mm}^2\cdot\text{day}^{-1}$
Diffusion coefficient of type 2 growth factors	D_{f2}	0.1	$\text{mm}^2\cdot\text{day}^{-1}$
The coefficient of chemotaxis along gradient of growth factors type 1	K_1	0.667	$\text{mm}^2\cdot\text{day}^{-1}\cdot\left(\frac{\text{ng}}{\text{mL}}\right)^{-1}$
The coefficient of chemotaxis along gradient of growth factors type 2	K_2	0.167	$\text{mm}^2\cdot\text{day}^{-1}\cdot\left(\frac{\text{ng}}{\text{mL}}\right)^{-1}$
Linear platelet taxis coefficient	H_T	0.333	$\text{mm}^2\cdot\text{day}^{-1}\cdot\mu\text{g}^{-1}$
The coefficient of platelet death due to inflammation	A_T	0.067	day^{-1}
The coefficient t of natural death of osteogenic cells	A_C	2×10^{-3}	day^{-1}
The coefficient of differentiation of osteoblasts into osteocytes	A_B	6.67×10^{-3}	day^{-1}
Natural decay rate of type 1 growth factors	A_{f1}	10	day^{-1}
Natural decay rate of type 2 growth factors	A_{f2}	10	day^{-1}
The coefficient of influence the concentration of adsorbed proteins on the secretion of growth factors of type 1	α_{T1}	6.67×10^{-5}	$\frac{\text{ng}}{\text{mL}}\cdot\text{day}^{-1}\cdot\left(\frac{\text{cells}}{\text{mL}}\right)^{-1}$

Table A1. *Cont.*

The coefficient of natural secretion of growth factors type 1	α_{T2}	10^{-5}	$\frac{\text{ng}}{\text{mL}} \cdot \text{day}^{-1} \cdot \left(\frac{\text{cells}}{\text{mL}}\right)^{-1}$
The coefficient of natural proliferation of osteogenic cells	α_{C0}	0.25	day^{-1}
The coefficient of enhancing the proliferation of osteogenic cells by growth factors	α_C	0.25	day^{-1}
The coefficient of influence of growth factors type 1 on the proliferation of osteoblasts	α_{CB}	0.5	day^{-1}
The coefficient of natural secretion of type 2 growth factors in the environment of osteogenic cells	α_{C2}	2.5×10^{-3}	$\frac{\text{ng}}{\text{mL}} \cdot \text{day}^{-1} \cdot \left(\frac{\text{cells}}{\text{mL}}\right)^{-1}$
The coefficient of natural secretion of type 2 growth factors in the environment of osteoblasts	α_{B2}	2.5×10^{-3}	$\frac{\text{ng}}{\text{mL}} \cdot \text{day}^{-1} \cdot \left(\frac{\text{cells}}{\text{mL}}\right)^{-1}$
The coefficient of influence of type 2 growth factors on bone synthesis	α_w	10^{-7}	$\text{day}^{-1} \cdot \left(\frac{\text{cells}}{\text{mL}}\right)^{-1}$
Bone remodeling coefficient (determined by numerical simulation to achieve v_l 09 within one year)	γ	-	-
Additional concentration of adsorbed proteins in the platelet environment	β_{T1}	0.1	$\mu\text{g} \cdot (\text{mm}^2)^{-1}$
Additional concentration of type 1 growth factors in the platelet environment	β_{T2}	10	$\text{ng} \cdot \text{mL}^{-1}$
Additional concentration of type 2 growth factors in the environment of osteogenic cells	β_{C2}	10	$\text{ng} \cdot \text{mL}^{-1}$
Additional concentration of type 2 growth factors in the environment of osteoblasts	β_{B2}	10	$\text{ng} \cdot \text{mL}^{-1}$
Additional concentration of growth factors affecting the proliferation of osteogenic cells	β_C	10	$\text{ng} \cdot \text{mL}^{-1}$
Additional concentration of growth factors affecting the proliferation of osteoblasts	β_{CB}	10	$\text{ng} \cdot \text{mL}^{-1}$
Additional concentration of type 2 growth factors affecting bone formation	β_w	10	$\text{ng} \cdot \text{mL}^{-1}$
Limiting cell density	N	10^6	$\text{cells} \cdot \text{mL}^{-1}$

* References to literary from which the parameter values are taken are given in [68].

References

1. Cieza, A.; Causey, K.; Kamenov, K.; Hanson, S.W.; Chatterji, S.; Vos, T. Global estimates of the need for rehabilitation based on the Global Burden of Disease study 2019: A systematic analysis for the Global Burden of Disease Study 2019. *Lancet* **2021**, *396*, 2006–2017. [[CrossRef](#)]
2. Popov, V.L.; Poliakov, A.M.; Pakhaliuk, V.I. Synovial Joints. Tribology, Regeneration, Regenerative Rehabilitation and Arthroplasty. *Lubricants* **2021**, *9*, 15. [[CrossRef](#)]
3. Mozgovaya, E.E.; Zborovskaya, I.A. Osteoarthritis is the most common joint disease. *Med. Her.* **2012**, *6*, 33–40.
4. Zhang, W.; Doherty, M.; Peat, G.; Bierma-Zeinstra, M.A.; Arden, N.K.; Bresnihan, B.; Herrero-Beaumont, G.; Kirschner, S.; Leeb, B.F.; Lohmander, L.S.; et al. EULAR evidence-based recommendations for the diagnosis of knee osteoarthritis. *Ann. Rheum. Dis.* **2010**, *69*, 483–489. [[CrossRef](#)] [[PubMed](#)]
5. Zhang, W.; Doherty, M.; Arden, N.; Bannwarth, B.; Bijlsma, J.; Gunther, K.P.; Hauselmann, H.J.; Herrero-Beaumont, G.; Jordan, K.; Kaklamanis, P.; et al. EULAR evidence based recommendations for the management of hip osteoarthritis: Report of a task force of the EULAR Standing Committee for International Clinical Studies Including Therapeutics (ESCISIT). *Ann. Rheum. Dis.* **2005**, *64*, 669–681. [[CrossRef](#)]
6. Lee, S.W.; Kim, W.Y.; Song, J.H.; Kim, J.H.; Lee, H.H. Factors Affecting Periprosthetic Bone Loss after Hip Arthroplasty. *Hip Pelvis* **2021**, *33*, 53–61. [[CrossRef](#)]
7. Krull, A.; Morlock, M.M.; Bishop, N.E. Factors influencing taper failure of modular revision hip stems. *Med. Eng. Phys.* **2018**, *54*, 65–73. [[CrossRef](#)]
8. Bijukumar, D.R.; Segu, A.; Souza, J.C.; Li, X.; Barba, M.; Mercuri, L.G.; Jacobs, J.J.; Mathew, M.T. Systemic and local toxicity of metal debris released from hip prostheses: A review of experimental approaches. *Nanomed. Nanotechnol. Biol. Med.* **2018**, *14*, 951–963. [[CrossRef](#)]
9. Liow, M.H.; Kwon, Y.M. Metal-on-metal total hip arthroplasty: Risk factors for pseudotumours and clinical systematic evaluation. *Int. Orthop.* **2017**, *41*, 885–892. [[CrossRef](#)]
10. Bijukumar, D.R.; Salunkhe, S.; Morris, D.; Segu, A.; Hall, D.J.; Pourzal, R.; Mathew, M.T. In vitro evidence for cell-accelerated corrosion within modular junctions of total hip replacements. *J. Orthop. Res.* **2020**, *38*, 393–404. [[CrossRef](#)]

11. Bijukumar, D.R.; Salunkhe, S.; Zheng, G.; Barba, M.; Hall, D.J.; Pourzal, R.; Mathew, M.T. Wear particles induce a new macrophage phenotype with the potential to accelerate material corrosion within total hip replacement interfaces. *Acta Biomater.* **2020**, *101*, 586–597. [[CrossRef](#)] [[PubMed](#)]
12. MacDonald, D.W.; Chen, A.F.; Lee, G.C.; Klein, G.R.; Mont, M.A.; Kurtz, S.M.; Taper Corrosion Writing Committee; Cates, H.E.; Kraay, M.J.; Rimnac, C.M. Fretting and Corrosion Damage in Taper Adapter Sleeves for Ceramic Heads: A Retrieval Study. *J. Arthroplast.* **2017**, *32*, 2887–2891. [[CrossRef](#)] [[PubMed](#)]
13. Smith, S.M.; Gilbert, J.L. Compliant interfaces and fretting corrosion of modular taper junctions in total hip implants: The micromechanics of contact. *Tribol. Int.* **2020**, *151*, 106437. [[CrossRef](#)]
14. Radzik, B.; Bijukumar, D.; Cheng, K.Y.; Badhe, R.V.; Barba, M.; Mathew, M.T. The role of fretting-frequency on the damage modes of THR modular junction: In-vitro study. *Mater. Sci. Eng. C Mater. Biol. Appl.* **2021**, *126*, 112128. [[CrossRef](#)]
15. Royhman, D.; Pourzal, R.; Hall, D.; Lundberg, H.J.; Wimmer, M.A.; Jacobs, J.; Hallab, N.J.; Mathew, M.T. Fretting-corrosion in hip taper modular junctions: The influence of topography and pH levels—An in-vitro study. *J. Mech. Behav. Biomed. Mater.* **2021**, *118*, 104443. [[CrossRef](#)]
16. Poliakov, A.; Pakhaliuk, V.; Popov, V. Current Trends in Improving of Artificial Joints Design and Technologies for Their Arthroplasty. *Front. Mech. Eng.* **2020**, *6*, 4. [[CrossRef](#)]
17. Goldman, A.H.; Sierra, R.J.; Trousdale, R.T.; Lewallen, D.G.; Berry, D.J.; Abdel, M.P. The Lawrence, D. Dorr surgical techniques & technologies award: Why are contemporary revision total hip arthroplasties failing? An analysis of 2500 cases. *J. Arthroplast.* **2019**, *34*, 11–16. [[CrossRef](#)]
18. Polyakov, A.; Pakhaliuk, V.; Kalinin, M.; Kramar, V.; Kolesova, M.; Kovalenko, O. System Analysis and Synthesis of Total Hip Joint Endoprosthesis. *Procedia Eng.* **2015**, *100*, 530–538. [[CrossRef](#)]
19. Chethan, K.N.; Shyamasunder Bhat, N.; Zuber, M.; Shenoy, S.B. Finite Element Analysis of Different Hip Implant Designs along with Femur under Static Loading Conditions. *J. Biomed. Phys. Eng.* **2019**, *9*, 507–516. [[CrossRef](#)]
20. Chethan, K.N.; Zuber, M.; Shyamasunder Bhat, N.; Shenoy, S.B. Optimized trapezoidal-shaped hip implant for total hip arthroplasty using finite element analysis. *Cogent Eng.* **2020**, *7*, 1719575. [[CrossRef](#)]
21. Kenney, C.; Dick, S.; Lea, J.; Liu, J.; Ebraheim, N.A. A systematic review of the causes of failure of revision total hip arthroplasty. *J. Orthop.* **2019**, *16*, 393–395. [[CrossRef](#)] [[PubMed](#)]
22. Khalifa, A.A.; Bakr, H.M. Updates in biomaterials of bearing surfaces in total hip arthroplasty. *Arthroplasty* **2021**, *3*, 32. [[CrossRef](#)]
23. Brown, A.S. Hip New World. *ASME Mech. Eng.* **2006**, *128*, 28–33. [[CrossRef](#)]
24. Bhaskar, B.; Arun, S.; Sreekanth, P.; Kanagaraj, S. Biomaterials in total hip joint replacements: The evolution of basic concepts, trends, and current limitations—A review. *Trends Biomater.* **2016**, *5*, 175–199. [[CrossRef](#)]
25. Khanna, R.; Ong, J.L.; Oral, E.; Narayan, R.J. Progress in Wear Resistant Materials for Total Hip Arthroplasty. *Coatings* **2017**, *7*, 99. [[CrossRef](#)]
26. Bingley, R.; Martin, A.; Manfredi, O.; Nejadhamzeeigilani, M.; Oladokun, A.; Beadling, A.R.; Siddiqui, S.; Anderson, J.; Thompson, J.; Neville, A.; et al. Fretting-corrosion at the modular tapers interface: Inspection of standard ASTM F1875-98. *Proc. Inst. Mech. Eng. H* **2018**, *232*, 492–501. [[CrossRef](#)]
27. Corne, P.; De March, P.; Cleymand, F.; Geringer, J. Fretting-corrosion behavior on dental implant connection in human saliva. *J. Mech. Behav. Biomed. Mater.* **2019**, *94*, 86–92. [[CrossRef](#)]
28. Geringer, J.; Macdonald, D. Friction/fretting-corrosion mechanisms: Current trends and outlooks for implants. *Mater. Lett.* **2014**, *134*, 52–157. [[CrossRef](#)]
29. Hemmerling, K.J.; Weitzler, L.; Bauer, T.W.; Padgett, D.E.; Wright, T.M. Fretting and corrosion of metal liners from modular dual mobility constructs: A retrieval analysis. *Bone Jt. J.* **2021**, *103-B*, 1238–1246. [[CrossRef](#)]
30. Fitz, D.W.; Klemm, C.; Chen, W.; Xiong, L.; Yeo, I.; Kwon, Y.-M. Head-Neck Taper Corrosion in Metal-on-Polyethylene Total Hip Arthroplasty: Risk Factors, Clinical Evaluation, and Treatment of Adverse Local Tissue Reactions. *J. Am. Acad. Orthop. Surg.* **2020**, *28*, 907–913. [[CrossRef](#)]
31. Fallahnezhad, K.; Feyzi, M.; Ghadirinejad, K.; Hashemi, R.; Taylor, M. Finite element based simulation of tribocorrosion at the head-neck junction of hip implants. *Tribol. Int.* **2022**, *165*, 107284. [[CrossRef](#)]
32. McLaughlin, J.R.; Lee, K.R.; Johnson, M.A. Second-generation uncemented total hip arthroplasty: A minimum 20-year follow-up. *Bone Jt. Open* **2021**, *2*, 33–39. [[CrossRef](#)] [[PubMed](#)]
33. McLaughlin, J.R.; Lee, K.R. Total Hip Arthroplasty with an Uncemented Tapered Femoral Component in Patients Younger than 50 Years of Age: A Minimum 20-Year Follow-Up Study. *J. Arthroplast.* **2016**, *31*, 1275–1278. [[CrossRef](#)] [[PubMed](#)]
34. Pourzal, R.; Lundberg, H.J.; Hall, D.J.; Jacobs, J.J. What Factors Drive Taper Corrosion? *J. Arthroplast.* **2018**, *33*, 2707–2711. [[CrossRef](#)]
35. Pilliar, R.M.; Cameron, H.U.; Macnab, I. Porous surface layered prosthetic devices. *Biomed. Eng.* **1975**, *10*, 126–131.
36. Pilliar, R.M. Powder metal-made orthopedic implants with porous surface for fixation by tissue ingrowth. *Clin. Orthop. Relat. Res.* **1983**, *176*, 42–51. [[CrossRef](#)]
37. Pilliar, R.M. Porous-surfaced metallic implants for orthopedic applications. *J. Biomed. Mater. Res.* **1987**, *21*, 1–33.
38. Owen, T.D.; Moran, C.G.; Smith, S.R.; Pinder, I.M. Results of uncemented porous-coated anatomic total hip replacement. *J. Bone Jt. Surg. Br.* **1994**, *76*, 258–262. [[CrossRef](#)]

39. Diaz-Dilernia, F.; Mansilla, A.M.G.; Forneris, A.A.; Slullitel, P.A.; Zanotti, G.; Comba, F.; Buttaro, F.P.M. Preliminary outcomes of the cementless UNITED hip system for primary total hip arthroplasty at a minimum 2-year follow-up. *Eur. J. Orthop. Surg. Traumatol.* **2021**. [[CrossRef](#)]
40. Kim, Y.H. Long-term results of the cementless porous-coated anatomic total hip prosthesis. *J. Bone Jt. Surg. Br.* **2005**, *87*, 623–627. [[CrossRef](#)]
41. Laine, H.J.; Puolakka, T.J.; Moilanen, T.; Pajamäki, K.J.; Wirta, J.; Lehto, M.U. The effects of cementless femoral stem shape and proximal surface texture on ‘fit-and-fill’ characteristics and on bone remodeling. *Int. Orthop.* **2000**, *24*, 184–190. [[CrossRef](#)] [[PubMed](#)]
42. Swider, P.; Pedrono, A.; Mouzin, O.; Søballe, K.; Bechtold, J.E. Biomechanical analysis of the shear behaviour adjacent to an axially loaded implant. *J. Biomech.* **2006**, *39*, 1873–1882. [[CrossRef](#)] [[PubMed](#)]
43. Moreo, P.; Perez, M.A.; Garcia-Aznar, J.M.; Doblare, M. Modelling the mechanical behaviour of living bony interfaces. *Comput. Meth. Appl. Mech. Eng.* **2007**, *196*, 3300–3314. [[CrossRef](#)]
44. Ambard, D.; Swider, P. A predictive mechano-biological model of the bone-implant healing. *Eur. J. Mech. A-Solids* **2006**, *25*, 927–937. [[CrossRef](#)]
45. Phillips, A.M. Overview of the fracture healing cascade. *Injury* **2005**, *36*, S5–S7. [[CrossRef](#)]
46. Gerstenfeld, L.C.; Cullinane, D.M.; Barnes, G.L.; Graves, D.T.; Einhorn, T.A. Fracture healing as a post-natal developmental process: Molecular, spatial, and temporal aspects of its regulation. *J. Cell Biochem.* **2003**, *88*, 873–884. [[CrossRef](#)]
47. Tsiridis, E.; Upadhyay, N.; Giannoudis, P. Molecular aspects of fracture healing: Which are the important molecules? *Injury* **2007**, *38*, S11–S25. [[CrossRef](#)]
48. Dimitriou, R.; Tsiridis, E.; Giannoudis, P.V. Current concepts of molecular aspects of bone healing. *Injury* **2005**, *36*, 1392–1404. [[CrossRef](#)]
49. Vermolen, F.J.; Javierre, E. A Suite of Continuum Models for Different Aspects in Wound Healing. In *Bioengineering Research of Chronic Wounds. Studies in Mechanobiology, Tissue Engineering and Biomaterials*; Gefen, A., Ed.; Springer: Berlin/Heidelberg, Germany, 2009; Volume 1. [[CrossRef](#)]
50. Sela, M.N.; Badihi, L.; Rosen, G.; Steinberg, D.; Kohavi, D. Adsorption of human plasma proteins to modified titanium surfaces. *Clin. Oral Implants Res.* **2007**, *18*, 630–638. [[CrossRef](#)]
51. Nygren, H.; Eriksson, C.; Lausmaa, J. Adhesion and activation of platelets and polymorphonuclear granulocyte cells at TiO₂ surfaces. *J. Lab. Clin. Med.* **1997**, *129*, 35–46. [[CrossRef](#)]
52. Cheung, A.; Phillips, A.M. Bone morphogenetic proteins in orthopaedic surgery. *Current Orthopaedics* **2006**, *20*, 424–429. [[CrossRef](#)]
53. Park, J.Y.; Gemmell, C.H.; Davies, J.E. Platelet interactions with titanium: Modulation of platelet activity by surface topography. *Biomaterials* **2001**, *22*, 2671–2682. [[CrossRef](#)]
54. Kikuchi, L.; Park, J.Y.; Victor, C.; Davies, J.E. Platelet interactions with calcium-phosphate-coated surfaces. *Biomaterials* **2005**, *26*, 5285–5295. [[CrossRef](#)] [[PubMed](#)]
55. Adair, T.H.; Montani, J.P. Angiogenesis. In *Overview of Angiogenesis*; Morgan & Claypool Life Sciences: San Rafael, CA, USA, 2010; Chapter 1. Available online: <https://www.ncbi.nlm.nih.gov/books/NBK53238/> (accessed on 1 December 2021).
56. Bikfalvi, A. Angiogenesis. *Encyclopedia of Endocrine Diseases*; Martini, L., Ed.; Elsevier: Amsterdam, The Netherlands, 2004; pp. 227–233. [[CrossRef](#)]
57. Linkhart, T.A.; Mohan, S.; Baylink, D.J. Growth factors for bone growth and repair: IGF, TGF beta and BMP. *Bone* **1996**, *19* (Suppl. 1), S1–S12. [[CrossRef](#)]
58. Pavlin, D.; Dove, S.B.; Zadro, R.; Gluhak-Heinrich, J. Mechanical loading stimulates differentiation of periodontal osteoblasts in a mouse osteoinduction model: Effect on type I collagen and alkaline phosphatase genes. *Calcif. Tissue Int.* **2000**, *67*, 163–172. [[CrossRef](#)]
59. Uto, Y.; Kuroshima, S.; Nakano, T.; Ishimoto, T.; Inaba, N.; Uchida, Y.; Sawase, T. Effects of mechanical repetitive load on bone quality around implants in rat maxillae. *PLoS ONE* **2017**, *12*, e0189893. [[CrossRef](#)]
60. Berglundh, T.; Abrahamsson, I.; Lindhe, J. Bone reactions to longstanding functional load at implants: An experimental study in dogs. *J. Clin. Periodontol.* **2005**, *32*, 925–932. [[CrossRef](#)]
61. Kuroshima, S.; Yasutake, M.; Tsuiki, K.; Nakano, T.; Sawase, T. Structural and Qualitative Bone Remodeling around Repetitive Loaded Implants in Rabbits. *Clin. Implant Dent. Relat. Res.* **2015**, *17*, e699–e710. [[CrossRef](#)]
62. Kitamura, E.; Stegaroiu, R.; Nomura, S.; Miyakawa, O. Biomechanical aspects of marginal bone resorption around osseointegrated implants: Considerations based on a three-dimensional finite element analysis. *Clin. Oral Implant. Res.* **2004**, *15*, 401–412. [[CrossRef](#)]
63. Assenza, B.; Scarano, A.; Petrone, G.; Iezzi, G.; Thams, U.; Roman, F.S.; Piattelli, A. Osteoclast activity around loaded and unloaded implants: A histological study in the beagle dog. *J. Oral Implantol.* **2003**, *29*, 1–7. [[CrossRef](#)]
64. Puleo, D.A.; Nanci, A. Understanding and controlling the bone-implant interface. *Biomaterials* **1999**, *20*, 2311–2321. [[CrossRef](#)]
65. Brunski, J.B. In vivo bone response to biomechanical loading at the bone/dental-implant interface. *Adv. Dent. Res.* **1999**, *13*, 99–119. [[CrossRef](#)] [[PubMed](#)]
66. Davies, J.E. Understanding peri-implant endosseous healing. *J. Dent. Educ.* **2003**, *67*, 932–949. [[CrossRef](#)] [[PubMed](#)]
67. Marco, F.; Milena, F.; Gianluca, G.; Vittoria, O. Peri-implant osteogenesis in health and osteoporosis. *Micron* **2005**, *36*, 630–644. [[CrossRef](#)] [[PubMed](#)]

68. Klein-Nulend, J.; Bacabac, R.G.; Bakker, A.D. Mechanical loading and how it affects bone cells: The role of the osteocyte cytoskeleton in maintaining our skeleton. *Eur. Cell Mater.* **2012**, *24*, 278–291. [[CrossRef](#)]
69. Bailón-Plaza, A.; van der Meulen, M.C. A mathematical framework to study the effects of growth factor influences on fracture healing. *J. Theor. Biol.* **2001**, *212*, 191–209. [[CrossRef](#)]
70. Geris, L.; Gerisch, A.; Maes, C.; Carmeliet, G.; Weiner, R.; Vander Sloten, J.; Van Oosterwyck, H. Mathematical modeling of fracture healing in mice: Comparison between experimental data and numerical simulation results. *Med. Biol. Eng. Comput.* **2006**, *44*, 280–289. [[CrossRef](#)]
71. Moreo, P.; García-Aznar, J.M.; Doblaré, M. Bone ingrowth on the surface of endosseous implants. Part 1: Mathematical model. *J. Theor. Biol.* **2009**, *260*, 1–12. [[CrossRef](#)]
72. Moreo, P.; García-Aznar, J.M.; Doblaré, M. Bone ingrowth on the surface of endosseous implants. Part 2: Theoretical and numerical analysis. *J. Theor. Biol.* **2009**, *260*, 13–26. [[CrossRef](#)]
73. Korzh, M.O.; Filipenko, V.A.; Radchenko, V.O.; Litvinov, L.A.; Voloshin, O.V.; Sliunin, Y.V.; Timchenko, I.B.; Golukhova, A.G.; Tankut, V.O.; Tankut, O.V. Hip Endoprosthesis. UA Patent 79,551, 25 June 2007.
74. Massin, P.; Lopes, R.; Masson, B.; Mainard, D. Does BioloX[®] Delta ceramic reduce the rate of component fractures in total hip replacement? *Orthop. Traumatol. Surg. Res.* **2014**, *100*, S317–S321. [[CrossRef](#)]
75. Koch, C.N.; Figgie, M.J.; Figgie, M.P.; Elpers, M.E.; Wright, T.M.; Padgett, D.E. Ceramic Bearings with Titanium Adapter Sleeves Implanted during Revision Hip Arthroplasty Show Minimal Fretting or Corrosion: A Retrieval Analysis. *HSS J.* **2017**, *13*, 241–247. [[CrossRef](#)] [[PubMed](#)]
76. Bouvet, J.C. Prosthesis Ball Joint. EP Patent 0,406,040, 1991.
77. Pakhaliuk, V.; Poliakov, A.; Fedotov, I. The ceramic modular head improvement in the design of a total hip replacement. *Facta Universitatis. Ser. Mech. Eng.* **2021**, *19*, 67–78. [[CrossRef](#)]
78. Kalin, B.A.; Fedotov, I.V.; Sevryukov, O.N.; Pakhalyuk, V.I.; Nemchinov, Y.M.; Ivannikov, A.A.; Suchkov, A.N. Method of soldered connection of alumina ceramic with titanium alloy BT1-0. RU Patent 2,717,446, 23 May 2020.
79. Carter, D.R.; Blenman, P.R.; Beaupré, G.S. Correlations between mechanical stress history and tissue differentiation in initial fracture healing. *J. Orthop. Res.* **1988**, *6*, 736–748. [[CrossRef](#)] [[PubMed](#)]
80. Palma, F.D.; Guignandon, A.; Chamson, A.; Lafage-Proust, M.H.; Laroche, N.; Peyroche, S.; Vico, L.; Rattner, A. Modulation of the responses of human osteoblast-like cells to physiologic mechanical strains by biomaterial surfaces. *Biomaterials* **2005**, *26*, 4249–4257. [[CrossRef](#)]
81. Raab-Cullen, D.M.; Thiede, M.A.; Petersen, D.N.; Kimmel, D.B.; Recker, R.R. Mechanical loading stimulates rapid changes in periosteal gene expression. *Calcif. Tissue Int.* **1994**, *55*, 473–478. [[CrossRef](#)]
82. Kobayashi, Y.; Hashimoto, F.; Miyamoto, H.; Kanaoka, K.; Miyazaki-Kawashita, Y.; Nakashima, T.; Shibata, M.; Kobayashi, K.; Kato, Y.; Sakai, H. Force-induced osteoclast apoptosis in vivo is accompanied by elevation in transforming growth factor b and osteoprotegerin expression. *J. Bone Miner. Res.* **2000**, *15*, 1924–1934. [[CrossRef](#)]